archives
of thermodynamics
Vol. **44**(2023), No. 1, 105–119
DOI: 10.24425/ather.2023.145879

A qualitative study of mixing a fluid inside a mechanical mixer with the effect of thermal buoyancy

SOUAD HASSOUNI[a]
HOUSSEM LAIDOUDI[b*]
OLUWOLE DANIEL MAKINDE[c]
MOHAMED BOUZIT[b]
BOUMEDIENE HADDOU[a]

[a] University of Science and Technology of Oran Mohamed-Boudiaf, Faculty of Chemistry, BP 1505, El-Menaouer, Oran, 31000, Algeria

[b] University of Science and Technology of Oran Mohamed-Boudiaf, Laboratory of Sciences and Marine Engineering, Faculty of Mechanical Engineering, BP 1505, El-Menaouer, Oran, 31000, Algeria

[c] Stellenbosch University, Faculty of Military Science, Private Bag X2, Saldanha 7395, South Africa

Abstract This paper is concerned with the rotational motion of the impeller and the thermal buoyancy within a mechanical mixer. The task was investigated numerically using the ANSYS-CFX simulator. The programmer is based on the finite volume method to solve the differential equations of fluid motion and heat transfer. The impeller has hot surfaces while the vessel has cold walls. The rotational movement of the impeller was controlled by the Reynolds number, while the intensity of the thermal buoyancy effect was controlled by the Richardson number. The equations were solved for a steady flow. After analyzing the results of this research, we were able to conclude that there is no effect of the values of Richardson number on the power number. Also, with the presence of the thermal buoyancy effect, the quality of the fluid mixing becomes more important. The increasing Richardson number increases the value of the Nusselt number of the impeller.

Keywords: Mechanical agitation; Mixing process; Heat transfer; Thermal buoyancy; Power number

*Corresponding Author. Email: houssem.laidoudi@univ-usto.dz

1 Introduction

The fluid mixing process is one of the important processes in the industry, and we mention the following: pharmaceutical products, food products such as chocolate, cosmetic products, milk products and so on. The fluid mixing process is usually carried out in a container of a certain geometric shape with a mechanical mixer inside it. The rotational motion of the impeller mixes the fluid. The quality of the mixture of the fluid depends mainly on the geometry of the impeller and the container (vessel), as well as the speed of rotation of the mixer.

A group of investigations have been aligned for the purpose of understanding the mixing process of the mechanical agitator, in order to arrive at the method that allows for increasing the mixing speed and decreasing the mechanical energy of the impeller. Among these important works, we mention the following. Hadjeb *et al.* [1] performed numerical research on a two-bladed agitator; this work was addressed for highly viscous fluids. Some geometrical changes of the mixer were made in order to increase the blending efficiency of the mixing process. Ameur studied the effect of the shape of the vessel on the mixing process. The impeller used in this work was that ofa six-curved-blade [2]. The studied shapes of the container were: a cylindrical vessel of flat bottom, cylindrical vessel of dished bottom and closed spherical vessel. The Herschel-Bulkley model was used to define the apparent viscosity of the fluid. The results showed that the last form of the vessel generated a uniform flow in the vessel. Ameur *et al.* [3] examined the hydrodynamic behaviour of highly viscous fluid in the mechanical agitator with the presence of a maxblend impeller. The investigations showed the effects of rotational speed, rheological characteristics and impeller clearance on the power consumption. Ameur and Bouzit simulated the rotation of a disc turbine impeller in the unbaffled vessel [4]. The working fluid was shear-thinning. It is a complex fluid whose dynamic viscosity depends on the shear rate. The results of this paper show the evolution of counter-rotating zones in the vessel with respect to pertinent parameters. Also, Ameur *et al.* investigated the mixing process for different shapes of impeller and vessel. The principal purpose of works [5–10] was to determine the best design of the impeller as well as of the vessel.

Cudak studied the agitation of a gas-liquid medium in a pseudophase system. The impeller of the mixing process was a Rushton turbine. The results of simulation were presented as contours of velocity and vectors [11]. Laidoudi presented a numerical work on a two-bladed impeller placed in an

unbaffled vessel [12]. Some new geometrical modifications were considered to improve the performance of the impeller. The results showed that the holed blades of the impeller are optimal. Foukrach *et al.* [13] simulated the turbulent flow in a cylindrical and polygonal vessel. The vessel in this research has vertical baffles. The $k-\varepsilon$ closure was used to model the turbulent flow. The results showed that the presence of vertical baffles in the vessel acts to improve the mixing process. Mishra *et al.* [14] simulated turbulent flow in a tank with a disc turbine. The work was to estimate rates of energy dissipation. Youcefi *et al.* [15] presented 3D simulations of turbulent flow in an unbaffled vessel. The purpose of the work was the estimation of the flow structure in the vessel. Torré *et al.* [16] presented experimental and numerical investigations of the impeller in an unbaffled vessel. Particle image velocimetry (PIV) was the experimental technique used for measuring the flow velocity. On the other hand, the standard $k-\varepsilon$ closure was also used to model the turbulent flow.

In addition to this, there are also some recently published papers [17–25], which on aggregate are hydrodynamic studies of the mixing process. The ultimate purpose of all these works is to reach a more efficient impeller that allows for speeding up the mixing process while reducing the consumption of mechanical energy. On other hand, thermal buoyancy can be defined as a force that allows hot fluid layers to move upwards, because they become less dense due to their high temperature. In fact, there is a group of papers that exploited this thermal property in enhancing thermal activity and controlling fluid movement such as [26–32].

In many industrial activities, we encounter the mixing process with the presence of heat transfer. However, after reviewing previous research papers in this field, it is clear that there is a lack of works that combine mechanical mixing and heat transfer. Therefore, through this work, we decided to support new findings in this area.

2 Geometrical description and mathematical modeling

Figure 1 shows the physical domain. It is formed of a cylindrical vessel (container) with a four-bladed impeller presented in Fig. 1a. Figure 1b shows the cross-section of the studied domain. The diameter of the vessel is given by D, while the diameter of the impeller is given d. The ratio between the two diameters is given as $d/D = 0.5$. The vessel also contains

four internal inflections. The radius of each cavity (e) is given by the ratio $e/D = 0.13$. Figure 1c shows the longitudinal view of the domain. The ratio between the height of the vessel (H) and its diameter is $H/D = 1$. The width of the blade of the impeller (a) is given by $a/D = 0.17$. The gap (c) between the flatted bottom of the vessel and the impeller is $c/D = 0.067$. The vessel is completely filled with a Newtonian fluid (water). However, the impeller surfaces have a high temperature (T_h) and the lateral walls of the vessel have a cold temperature (T_c). The flatted bottom and the top of the vessel have an adiabatic condition.

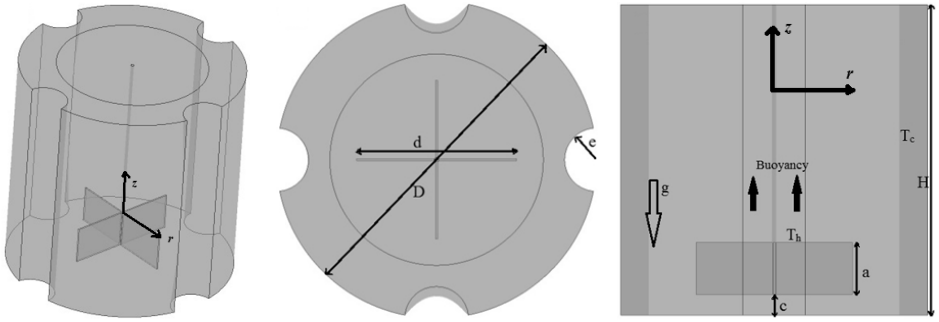

(a) (b) (c)

Figure 1: The studied domain: a) general view, b) cross-section view, c) longitudinal view.

We note that the rotation of the impeller creates a flow inside the vessel, and these results generate the forced convection heat transfer. On the other hand, the gradient temperature between the impeller and vessel surfaces generates a natural convection heat transfer. Together we get the mixed convection.

The Reynolds number controls the rotational speed of the impeller as

$$\mathrm{Re} = \frac{\rho N D^2}{\mu}\,, \tag{1}$$

where ρ, N, and μ are the fluid density, rotational speed, and dynamic viscosity, respectively.

The Prandtl number defines the thermophysical proprieties of the fluid:

$$\mathrm{Pr} = \frac{\vartheta cp}{k}\,, \tag{2}$$

where υ, cp, and k are the kinematic viscosity, heat capacity of the fluid, and thermal conductivity, respectively. Indeed, $\mathrm{Pr} = 6.01$ in this paper.

The Richardson number defines the intensity of thermal buoyancy.

$$\mathrm{Ri} = \frac{g\beta_T \Delta T D^3}{(ND)^2}\,, \tag{3}$$

where g and β_T are the gravitational acceleration and dilatation coefficient of the fluid, and $\Delta T = (T_h - T_c)$ is the difference in temperature between the hot temperature of the impeller surfaces and a cold temperature of the lateral walls of the vessel.

The power number characterizes the consumption power and is given as:

$$\mathrm{Np} = \frac{P}{\rho N^3 D^5}\,, \tag{4}$$

where P is the mechanical power and it is calculated as a volume integral:

$$P = \mu \int\limits_{\text{vessel\_volume}} Q_v \, dv, \tag{5}$$

where Q_v denotes viscous dissipation. For the cylindrical coordinate system (r, θ, z) dv is expressed in the form

$$dv = r \, dr \, d\theta \, dz, \tag{6}$$

and we have

$$Q_v = \frac{1}{\mu^2}\left(2\tau_{rr}^2 + 2\tau_{\theta\theta}^2 + 2\tau_{zz}^2 + 2\tau_{rz}^2 + 2\tau_{r\theta}^2 + 2\tau_{z\theta}^2\right), \tag{7}$$

where

$$\tau_{rr} = -2\mu\left(\frac{\partial v_r}{\partial r}\right), \tag{8}$$

$$\tau_{r\theta} = -\mu\left[r\frac{\partial\left(v_\theta/r\right)}{\partial r} + \frac{1}{r}\frac{\partial v_r}{\partial \theta}\right], \tag{9}$$

$$\tau_{rz} = -\mu\left[\frac{\partial v_r}{\partial z} + \frac{\partial v_z}{\partial r}\right]. \tag{10}$$

The average Nusselt number of the impeller is calculated through the integration of the local Nusselt number (Nu_L) over all impeller surfaces (A) as

$$\mathrm{Nu} = \frac{1}{A}\int \mathrm{Nu}_L \, dA, \tag{11}$$

where

$$\mathrm{Nu}_L = \left(\frac{\partial \theta}{\partial n_s}\right)_{\text{wall}} \tag{12}$$

and n_s is the normal unit vector.

3 Simulation steps

Gambit was used for the design and generation of the mesh grid. The grid has unstructured elements with non-uniform distribution as shown in Fig. 2. The concentration of elements is around the impeller. The number of meshing elements was selected after the grid independence test. The results of the grid independence test are presented in Table 1. It is clear that grid G2 is sufficient for the present computation, because the difference between this grid (G2) and the third one (G3) is very small (around 0.12%).

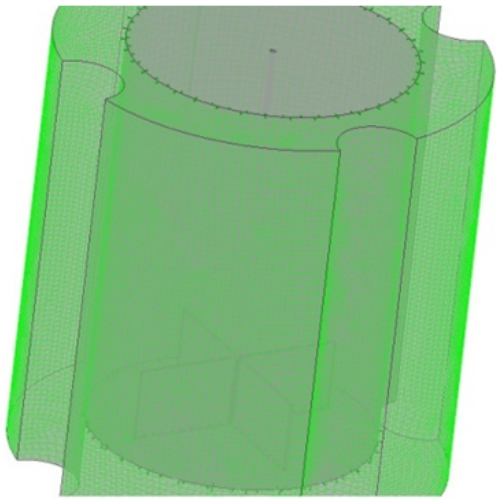

Figure 2: Grid quality for the studied domain.

Table 1: Results of grid independence test, for Re = 30, Ri = 0 and Pr = 6.01

Case	Elements	Np	Variation, %
G 1	231.500	0.006945	7.79
G 2	463.000	0.007532	0.12
G 3	926.000	0.007541	–

The simulations were carried out using the finite volume method (ANSYS-CFX simulator [33]). The SIMPLEC (semi-implicit method for pressure linked equations-consistent) algorithm was used for coupling pressure and velocity. Meanwhile, the high-resolution discretisation scheme was used for solving the convective term. The relative errors of the computations are

10^{-8} for the continuity and momentum equations and 10^{-6} for the energy equation. Furthermore, the multi-reference frame (MRF) method was used for this simulation [33]. The inner impeller was created in the rotating domain, while the rest of the domain was selected fixed.

In this section, the validation test is described where the present numerical methodology has been proofed. The results of the validation test are shown in Fig. 3. Indeed, a good agreement is shown between our results and the results of Ameur *et al.* [9]. The notable difference between the results of our simulation (present data) and the previous work (Ameur *et al.* [9]) is due to the uncertainty involved in the method used in the calculation of correlation of Ameur *et al.*

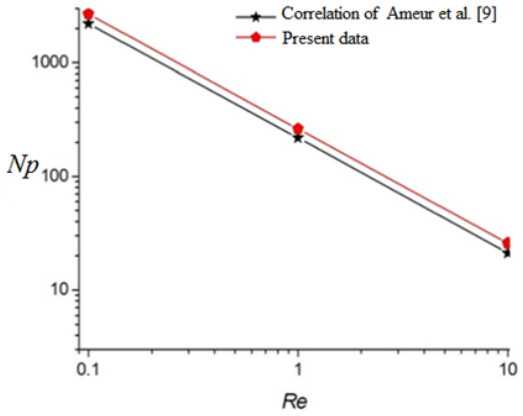

Figure 3: Validation test.

4 Results and discussion

The results of this work include mechanical agitation and mixed convection heat transfer for a fluid inside a cylindrical vessel. The vessel has four cavities of a semi-circular shape and a flat base. However, the impeller has also four blades. The purpose of this research is to predict the movement of the fluid inside the vessel due to the rotation of the impeller.

Figure 4 presents the dimensionless velocity distribution over the cross-section of height $Z = 0.35$ as defined in relation to the total height of the vessel ($Z = z/H$). The flow velocity is made dimensionless with respect to speed rotation of the impeller. Figure 4 shows the effect of the rotational speed of the impeller on the movement of the fluid without the effect of

thermal buoyancy (Ri = 0). It is clear that the maximum value of the velocity is at the head of the blades while it gradually decreases as we move towards the wall of the vessel from the centre of the impeller. It is also noted that there is no noticeable influence of the studied values of the Reynolds number on the fluid motion.

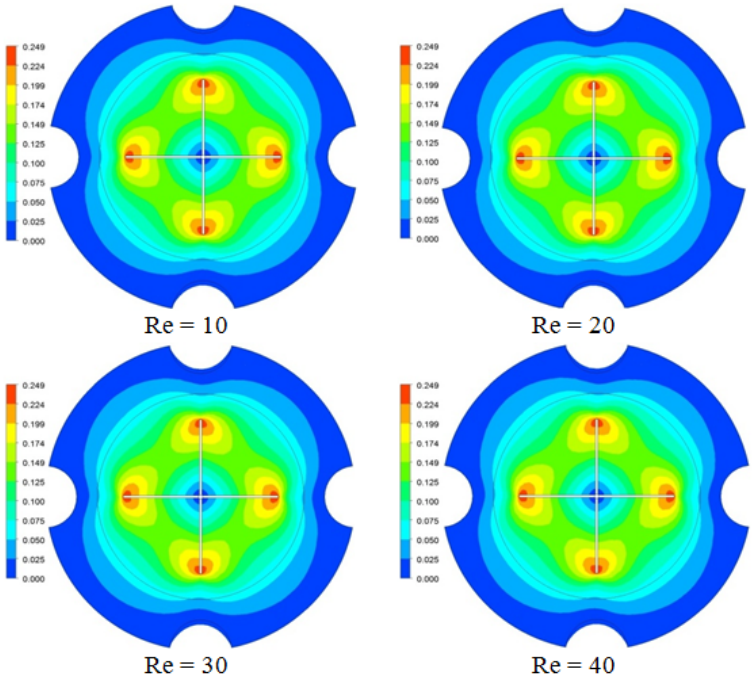

Figure 4: Contours of dimensionless velocity for different Re at Ri = 0.

Figure 5 shows the gradual effect of thermal buoyancy on the dynamic behaviour of the flow for a constant value of Reynolds number (Re = 40). Increasing the value of Richardson number indicates an increase in the thermal buoyancy effect. Figure 5 illustrates the variation in velocity distribution in the same section as in Fig. 4. We note that the higher the value of Ri, the greater the flow velocity. It can be concluded that the fluid movement is very important in this case, which makes the fluid mixing process better and faster.

Figure 6 exhibits the dimensionless velocity distribution contours for different Richardson numbers in the longitudinal section of the vessel with the impeller at Re = 40. Note that in the case Ri = 0, the velocity diffusion is

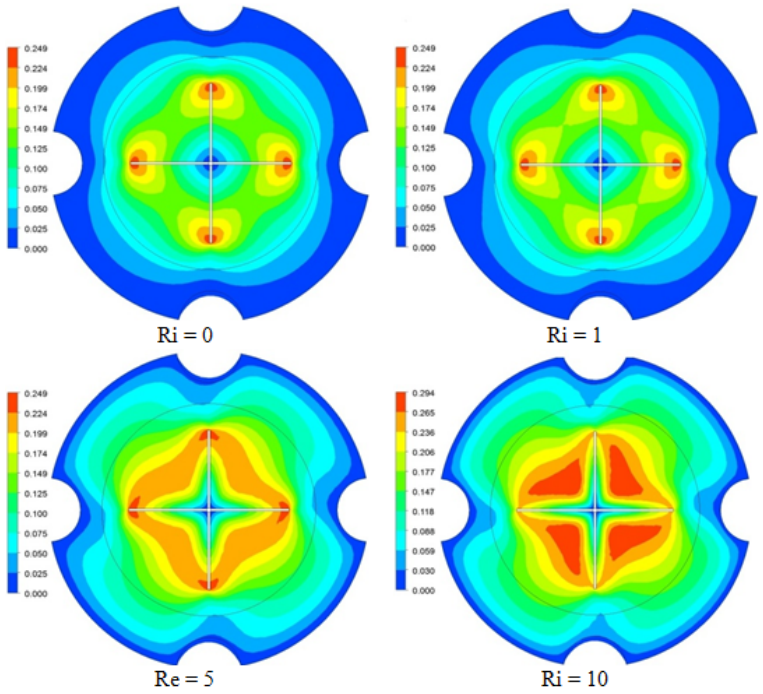

Figure 5: Contours of dimensionless velocity for different Ri at Re = 40.

only at the bottom near the impeller blades. Whereas, the higher the value of the Richardson number, the greater the velocity spread to the top. This phenomenon is explained by the following: the fact that the mixer is hot is what pushes the hot fluid particles upward, and this is what makes the fluid velocity increasing with (increasing) Richardson number. It is also noted from Fig. 6 that the mixing process of the fluid due to the thermal buoyancy phenomenon is very significant compared to the mechanical mixing of the impeller.

Figures 7 and 8 show the isotherms for different Ri and for Re = 40. Figure 7 forms a cross-sectional view at the height $Z = 0.35$, whereas Figure 8 is a longitudinal view of isotherms. It is clear that the dissipation of gradient temperature around the impeller decreases with the increasing Richardson number, which means that the temperature gradient becomes important with the increasing Richardson number. So, we can predict that the heat transfer between the impeller and the fluid increases gradually with the increasing Richardson number. It appears clear from Fig. 7 that

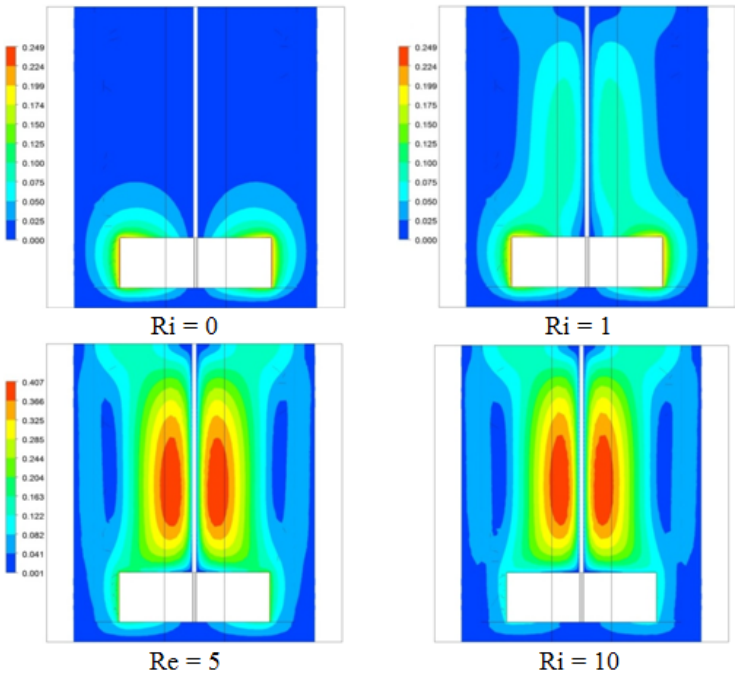

Figure 6: Contours of dimensionless velocity for different Ri at Re = 40 (longitudinal section).

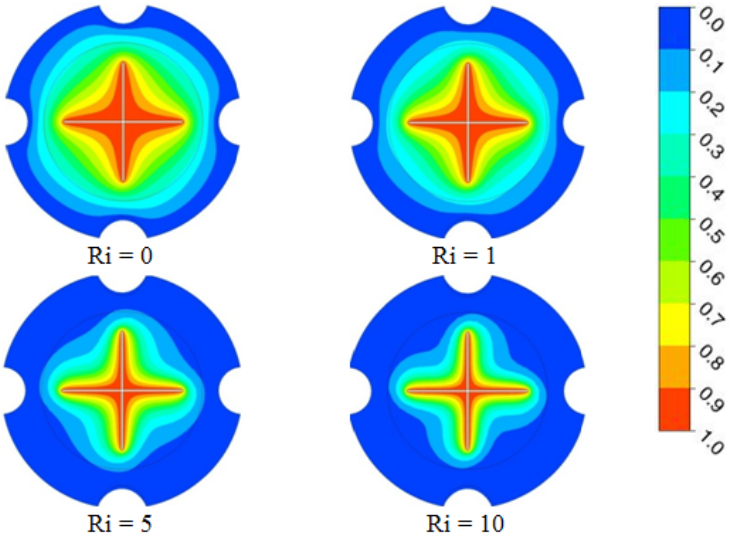

Figure 7: Isotherms (dimensionless temperature) at cross-section Z = 0.35 for different Ri for Re = 40.

the lower side of the impeller experiences a larger rate of heat transfer as compared to the upper side. In addition to this, it can be seen that the fluid motion intensifies with increasing thermal buoyancy and this confirms the previous results.

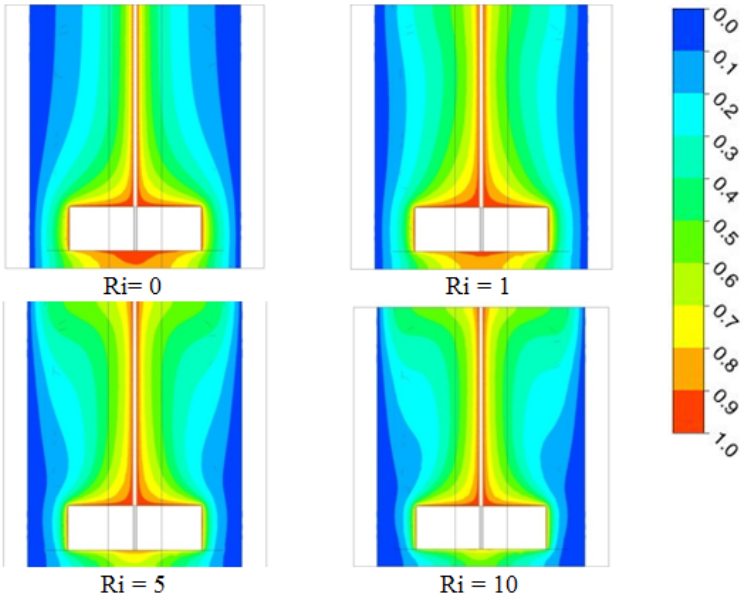

Figure 8: Longitudinal view of isotherms (dimensionless temperature) for different Ri for Re = 40.

Figure 9 presents the variation of the dimensionless velocity component W along the radius of the vessel at the height $Z = 0.5$. The first thing that can be seen is that the velocity W increases with the increasing value of Richardson number. Near the impeller, the velocity sign is positive, that is the flow is directed upwards, while near the vessel wall, the velocity sign is negative, meaning that the direction of the flow is downward. It is also noted that the value of the maximum velocity of the upward flow is much greater than the value of the maximum velocity of the downward flow.

Figure 10 shows the variation of power number with Reynolds number and Richardson number. It is clear that increasing the Reynolds number decreases the value of power number. On the other hand, there is no change in the power number with respect to the Richardson number. This confirms that there is no effect of thermal buoyancy on the mechanical energy of the impeller.

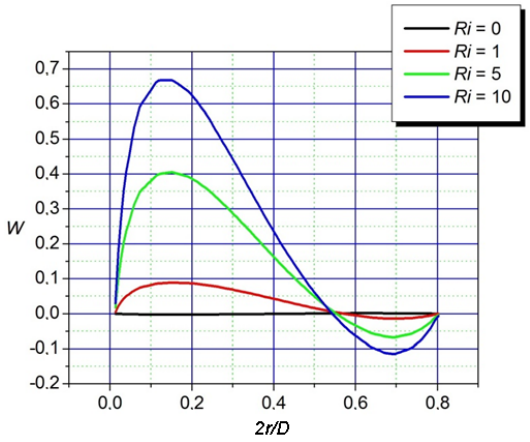

Figure 9: Dimensionless velocity along the vessel radius as a function of Ri for Re = 40.

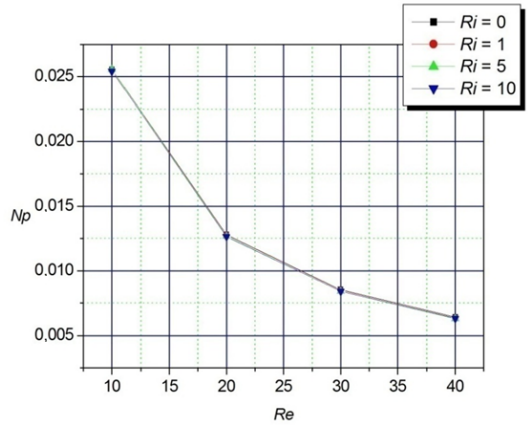

Figure 10: Variation of power number *versus* Re and Ri.

Figure 11 shows the evolution of the Nusselt number with the Richardson and Reynolds numbers. Note that since the heat transfer is of the forced convection type (Ri = 0), raising the Reynolds number does not effectively influence the value of the Nusselt number. On the other hand, in the mixed-type heat transfer (Ri $\neq$ 0), raising the value of the Reynolds number positively affects the value of the Nusselt number. It is noted that the effect of Reynolds number on Nusselt number is large whenever the value of Richardson number is significant.

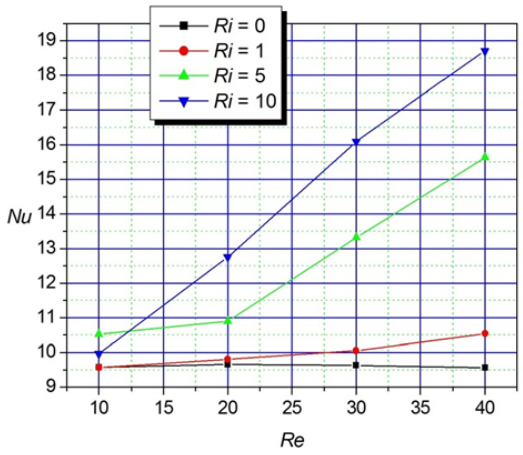

Figure 11: Variation of Nusselt number *versus* Re and Ri.

5 Summary

The research is concerned with 3D numerical simulation of a mechanical agitator. The impeller is a four-bladed turbine. The impeller has an elevated temperature while the vessel is cold. The impeller rotates at a constant speed. The purpose of this research is to study the effect of the impeller rotation speed and the thermal buoyancy factor on fluid motion in the vessel. After studying and analyzing the results, we have reached the following conclusions:

- Fluid motion within the vessel is intensified after the thermal buoyancy effect is added.
- When Ri = 0, increasing the Reynolds number does not affect the value of Nusselt number.
- The higher the value of Richardson number, the greater the effect of the value of Reynolds number on Nusselt number.
- With the presence of the thermal buoyancy effect, the quality of the fluid mixing is significantly increased.
- There is no effect of Richardson number on the power number.

Through the results of this work, we can suggest some new conditions for the intensification of the mixing process: such as the use of some complex fluids or the change in the configuration of the hot spots inside the vessel.

Received 16 February 2023

References

[1] Hadjeb A., Bouzit M., KamlaY., Ameur H.: *A new geometrical model for mixing of highly viscous fluids by combining two-blade and helical screw agitators.* Pol. J. Chem. Technol. **19**(2017), 83–91.

[2] Ameur H.: *Agitation of yield stress fluids in different vessel shapes.* Eng. Sci. Technol. Int. J. **19**(2016), 189–196.

[3] Ameur H., Bouzit M., Helmaoui M.: *Hydrodynamic study involving a maxblend impeller with yield stress fluids.* J. Mech. Sci. Technol. **26**(2012), 1523–1530.

[4] Ameur H., Bouzit M.: *Numerical investigation of flow induced by a disc turbine inunbaffled stirred tank.* Acta Sci. **35**(2013), 469-476.

[5] Ameur H., Bouzit M.: *3D hydrodynamics and shear rates variability in the United-States Pharmacopeia paddle dissolution apparatus.* Int. J. Pharm. **452**(2013), 42–51.

[6] Ameur H., Bouzit M., Ghenaim A.: *Numerical study of the performance of multistage Scaba 6SRGT impellers for the agitation of yield stress fluids in cylindrical tanks.* J. Hydrodyn. Ser. B **27**(2015), 3, 436–442.

[7] Ameur H., Sahel D., Kamla Y.: *Energy efficiency of a deep hollow bladed impeller for mixing viscoplastic fluids in a cylindrical vessel.* Adv. Mech. Eng. **9**(2017), 1–7.

[8] Ameur H., Kamla Y., Sahel D.: *Optimization of the operating and design conditions to reduce the power consumption in a vessel stirred by a paddle impeller.* Period. Polytech. Mech. Eng. **62**(2018), 312–319.

[9] Ameur H., Bouzit M.: *Power consumption for stirring shear thinning fluids by two-blade impeller.* Energy **50**(2013), 326–332.

[10] Ameur H., Bouzit M., Helmaoui M.: *Numerical study of fluid flow and power consumption in a stirred vessel with a Scaba 6SRGT impeller.* Chem. Process Eng. **32**(2011), 351–366.

[11] Cudak M.: *Numerical analysis of hydrodynamics in a mechanically agitated gas-liquid pseudophase system.* Chem. Pap. **73**(2018), 481–489.

[12] Laidoudi H.: *Hydrodynamic analyses of the flow patterns in stirred vessel of two bladed impeller.* J. Serb. Soc. Comput. Mech. **14**(2020), 117–132.

[13] Foukrach M., Bouzit M., Ameur H., Kamla Y.: *Influence of the vessel shape on the performance of a mechanically agitated system.* Chem. Pap. **73**(2018), 469–480.

[14] Mishra V.P., Kumar P., Joshi J.B.: *Flow generated by a disc turbine in aqueous solutions of polyacrylamide.* Chem. Eng. J. **71**(1998), 11–21.

[15] Youcefi S., Bouzit M., Ameur H., Kamla Y., Youcefi A.: *Effect of some design parameters on the flow fields and power consumption in a vessel stirred by a Rushton turbine.* Chem. Process Eng. **34**(2013), 293–307.

[16] Torre J.P., Fletcher D.F., Lasuye T., Xuereb C.: *Single and multiphase CFD approaches for modelling partially baffled stirred vessels: Comparison of experimental data with numerical predictions.* Chem. Eng. Sci. **62**(2007), 6246–6262.

[17] Heidari A.: *CFD simulation of impeller shape effect on quality of mixing in two-phase gas-liquid agitated vessel*. Chinese J. Chem. Eng. **28**(2020), 2733–2745.

[18] Ghotli R.A., Shafeeyan M.S., Abbasi M.R., Ramand A.A.A., Ibrahim S.: *Macromixing study for various designs of impellers in a stirred vessel*. Chem. Eng. Process. – Process Intensific. **148(**2020), 107794.

[19] Ghotli R.A.R, Abbas M.R., Bagheri A.H., Raman A.A.A., Ibrahim S., Bostanci H.: *Experimental and modeling evaluation of droplet size in immiscible liquid-liquid stirred vessel using various impeller designs*. J. Taiwan Inst. Chem. Eng. **100**(2019), 26–36.

[20] Yamamoto T., Fang Y., KomarovS.V.: *Surface vortex formation and free surface deformation in an unbaffled vessel stirred by on-axis and eccentric impellers*. Chem. Eng. J. **367**(2019), 25–36.

[21] Yang F., Zhou S., An X.: *Gas-liquid hydrodynamics in a vessel stirred by dual dislocated-blade Rushton impellers*. Chinese J. Chem. Eng. **23**(2015), 1746–1754.

[22] Magelli F., Montante G., Pinelli D., Paglianti A.: *Mixing time in high aspect ratio vessels stirred with multiple impellers*. Chem. Eng. Sci. **101**(2013), 712–720.

[23] Takahashi K., Motoda M.: *Chaotic mixing created by object inserted in a vessel agitated by an impeller*. Chem. Eng. Res. Des. **87**(2009), 386–390.

[24] Cudmore G.C., Holloway A.G.L., Gerber A.G.: *A model of impeller whirl for baffled mixing vessels*. J. Fluid. Struct. **54**(2015), 719–742.

[25] Woziwodzki S.: *Mixing of viscous Newtonian fluids in a vessel equipped with steady and unsteady rotating dual-turbine impellers*. Chem. Eng. Res. Des. **92**(2014), 3, 435–446.

[26] Laidoudi H.: *Enhancement of natural convection heat transfer in concentric annular space using inclined elliptical cylinder*. J. Nav. Arch. Mar. Eng. **17**(2020), 89–99.

[27] Aliouane I., Kaid N., Ameur H., Laidoudi H.: *Investigation of the flow and thermal fields in square enclosures: Rayleigh-Bénard's instabilities of nanofluids*. Therm. Sci. Eng. Prog. **25**(2021), 100959.

[28] Laidoudi H., Bouzit M.: *The effects of aiding and opposing thermal buoyancy on downward flow around a confined circular cylinder*. Period. Polytech. Mech. Eng. **62**(2018), 42–50.

[29] Godoy T.: *Singular elliptic problems with Dirichlet or mixed Dirichlet-Neumann non-homogeneous boundary conditions*. Opuscula Math. **43**(2023), 19–46.

[30] Szymański P., Mikielewicz D.: *Challenges in operating and testing loop heat pipes in 500–700 K temperature ranges*. Arch. Thermodyn. **43**(2022), 2, 61–73.

[31] Cyklis P.: *Heat transfer in falling film evaporators during the industrial process of apple juice concentrate production*. Arch. Thermodyn. **39**(2018), 3, 3–13.

[32] Bulat P.V., Volkov K. N.: *Fluid/solid coupled heat transfer analysis of a free rotating disc*. Arch. Thermodyn. **39**(2018), 3, 169–192.

[33] ANSYS-CFX. https://www.ansys.com/products/fluids/ansys-cfx (acessed 11 Aug. 2022).